

AD-A225 837

DTIC FILE COPY

①

OFFICE OF NAVAL RESEARCH

Contract N00014-82K-0612

Task No. NR 627-838

TECHNICAL REPORT NO. 50

Ion-Transporting Composite Membranes.
III. Selectivity and Rate of Ion Transport
in Nafion[®]-Impregnated Gore-Tex Membranes Prepared
By a High Temperature Solution-Casting Method

by

Chao Liu and Charles R. Martin

Prepared for publication

in

Journal of Electrochemical Society

Department of Chemistry
Colorado State University
Ft. Collins, CO 80523

August 2, 1990

Reproduction in whole or in part is permitted for
any purpose of the United States Government

*This document has been approved for public release
and sale; its distribution is unlimited

*This statement should also appear in Item 10 of Document
Control Data - DD Form 1473. Copies of form
Available from cognizant contract administrator

DTIC
ELECTE
AUG 17 1990
S B D

90 08 17 074

REPORT DOCUMENTATION PAGE

Form Approved
OMB No. 0704-0188

1a. REPORT SECURITY CLASSIFICATION UNCLASSIFIED			1b. RESTRICTIVE MARKINGS		
2a. SECURITY CLASSIFICATION AUTHORITY			3. DISTRIBUTION / AVAILABILITY OF REPORT APPROVED FOR PUBLIC DISTRIBUTION, DISTRIBUTION UNLIMITED.		
2b. DECLASSIFICATION / DOWNGRADING SCHEDULE					
4. PERFORMING ORGANIZATION REPORT NUMBER(S) ONR TECHNICAL REPORT # 50			5. MONITORING ORGANIZATION REPORT NUMBER(S)		
6a. NAME OF PERFORMING ORGANIZATION Dr. Charles R. Martin Department of Chemistry		6b. OFFICE SYMBOL (if applicable)		7a. NAME OF MONITORING ORGANIZATION Office of Naval Research	
6c. ADDRESS (City, State, and ZIP Code) Colorado State University Ft. Collins, CO 80523		7b. ADDRESS (City, State, and ZIP Code) 800 North Quincy Street Arlington, VA 22217			
8a. NAME OF FUNDING / SPONSORING ORGANIZATION Office of Naval Research		8b. OFFICE SYMBOL (if applicable)		9. PROCUREMENT INSTRUMENT IDENTIFICATION NUMBER Contract # N00014-82K-0612	
8c. ADDRESS (City, State, and ZIP Code) 800 North Quincy Street Arlington, VA 22217		10. SOURCE OF FUNDING NUMBERS			
		PROGRAM ELEMENT NO.	PROJECT NO.	TASK NO.	WORK UNIT ACCESSION NO.
11. TITLE (Include Security Classification) Ion-Transporting Composite Membranes. III. Selectivity and Rate of Ion Transport in Nafion ^R -Impregnated Gore-Tex Membranes Prepared By a High Temperature Solution-Casting Method					
12. PERSONAL AUTHOR(S) Chao Liu and Charles R. Martin					
13a. TYPE OF REPORT Technical		13b. TIME COVERED FROM _____ TO _____		14. DATE OF REPORT (Year, Month, Day) (90, 08, 02) Aug. 2, 1990	
15. PAGE COUNT					
16. SUPPLEMENTARY NOTATION					
17. COSATI CODES			18. SUBJECT TERMS (Continue on reverse if necessary and identify by block number)		
FIELD	GROUP	SUB-GROUP	Composite membranes, Nafion/Gore-Tex, ion-transport		
19. ABSTRACT (Continue on reverse if necessary and identify by block number) In a previous paper we discussed the rate of ion-transport in Nafion Impregnated Gore-Tex (NIGT) membranes. The membranes described in this previous paper were prepared by immersing the Gore-Tex in a solution of Nafion and then allowing the solvent to evaporate at room temperature. Nafion films which are cast at room temperature show poor mechanical and transport properties. This paper describes the transport properties of NIGT membranes prepared via a high temperature solution-casting method. We have found that these high temperature-cast NIGT membranes show better physical and mechanical properties than the low temperature-cast NIGT investigated previously. The two diffusion-pathway model, described in the previous paper, quantitatively accounts for the transport data for the high temperature-cast membranes. At the ca. 10 percent (or higher) Nafion loading-level, both the high and low temperature-cast membranes show excellent cation permselectivity. Furthermore these membranes show cation-transport rates for $\text{Ru}(\text{NH}_3)_6^{3+}$ which are an order of magnitude higher than transport rates in homogeneous Nafion.					
20. DISTRIBUTION / AVAILABILITY OF ABSTRACT <input checked="" type="checkbox"/> UNCLASSIFIED/UNLIMITED <input type="checkbox"/> SAME AS RPT. <input type="checkbox"/> DTIC USERS			21. ABSTRACT SECURITY CLASSIFICATION		
22a. NAME OF RESPONSIBLE INDIVIDUAL Dr. Robert Nowak			22b. TELEPHONE (Include Area Code) (202) 696-4410		22c. OFFICE SYMBOL

Abstract

In a previous paper we discussed the rate of ion-transport in Nafion Impregnated Gore-Tex (NIGT) membranes. The membranes described in this previous paper were prepared by immersing the Gore-Tex in a solution of Nafion and then allowing the solvent to evaporate at room temperature. Nafion films which are cast at room temperature show poor mechanical and transport properties.

This paper describes the transport properties of NIGT membranes prepared via a high temperature solution-casting method. We have found that these high temperature-cast NIGT membranes show better physical and mechanical properties than the low temperature-cast NIGT investigated previously. The two diffusion-pathway model, described in the previous paper, quantitatively accounts for the transport data for the high temperature-cast membranes. At the ca. 10 percent (or higher) Nafion loading-level, both the high and low temperature-cast membranes show excellent cation permselectivity. Furthermore these membranes show cation-transport rates for $\text{Ru}(\text{NH}_3)_6^{3+}$ which are an order of magnitude higher than transport rates in homogeneous Nafion.



Accession For	
NTIS GRA&I	<input checked="checked" type="checkbox"/>
DTIC TAB	<input type="checkbox"/>
Unannounced	<input type="checkbox"/>
Justification	
By	
Distribution/	
Availability Codes	
Dist	Avail and/or Special
A-1	

INTRODUCTION

We have been investigating the transport properties of ionically conductive composite polymer membranes (1,2). These composites are prepared by doping an inert, microporous host membrane with an ion exchange polymer (1,2). Our investigations have focused on composites prepared by incorporating Nafion[®], a perfluorosulfonate ion exchange polymer (3), into Gore-tex, a microporous polytetrafluoroethylene filtration membrane.

In our previous studies, the Nafion-impregnated Gore-tex (NIGT) membranes were prepared by immersing Gore-tex into a Nafion solution and then allowing the solvent to evaporate at room temperature (1,2). Our fundamental investigations of the properties of solution-cast Nafion have shown, however, that Nafion films which are cast at room temperature have poor mechanical properties and low cation permselectivities (4-5); Redepenning and Anson have shown that these low temperature-cast films have low cation permselectivities (6). In contrast, Nafion films which are cast at elevated temperatures (greater than ca. 150° C) have good mechanical properties and high cation permselectivities (4-6). These high temperature solution-cast films are essentially identical to as-received Nafion.

These fundamental investigations of solution-cast Nafion suggested to us that NIGT membranes prepared at elevated temperatures might have superior mechanical and transport properties. We have prepared a series of NIGT membranes using a high temperature solvent evaporation procedure. Electrochemical methods (7-9) were used to evaluate cation-transport rates in these new NIGT membranes. We have also used a potentiometric method (10) to conduct the first studies of cation permselectivity of NIGT.

We have found that these new NIGT membranes can be nearly as cation permselective as Nafion; these membranes can also support much higher rates of cation-transport than Nafion. We report the results of these investigations in this paper.

EXPERIMENTAL

Materials. Nafion 117 (1100 equivalent weight, proton form) was obtained from du Pont. Dimethylsulfoxide (DMSO) and ethanol/water solutions of Nafion were prepared using the procedures of Martin et al. (4,11). Gore-tex filtration membranes (20 nm and 200 nm mean pore diameter) were donated by W.L. Gore and Associates. $\text{Ru}(\text{NH}_3)_6\text{Cl}_3$ was purchased from Johnson Matthey. Purified water was obtained by passing house distilled water through a Milli-Q (Millipore) water purification system. All other reagents were of the highest purity available and were used without further purification.

Instrumentation. Rotating disk voltammetry was conducted using a Pine Instruments AFSA-2 electrode rotator in conjunction with an EG&G PARC 273 potentiostat/galvanostat. The PARC 273 was controlled by an IBM XT personal computer. The experimental data were saved in ASCII files and transferred to the spreadsheet Lotus 123.

Electrodes and electrochemical cells. Cation-transport rates in the NIGT membranes were evaluated using rotating NIGT-covered Pt disk electrodes. These electrodes were prepared by stretching NIGT membranes over the face of a 0.7 cm-dia. Pine Instruments rotating Pt disk electrode. The NIGT membranes were held in place with a collar of heat-shrinkable Teflon tubing (1,2,12). The Pt surface was polished as described previously (12).

A three-compartment electrochemical cell was used for the rotating NIGT-covered electrode studies. The reference compartment housed a saturated

calomel reference electrode (SCE) and was connected to the main (working electrode) compartment via a Luggin capillary. The counter electrode compartment housed a Pt flag counter electrode and was connected to the main compartment via a glass frit. The entire assembly was immersed in a constant temperature water bath maintained at $25.0 \pm 0.1^\circ \text{C}$. All potentials are reported vs. SCE.

Selectivity of cation transport in the NIGT membranes was evaluated potentiometrically (10); a schematic diagram of the cell used is shown in Figure 1. The NIGT membrane separates two Teflon half cells. The half cells are held together using the vise-type cell holder shown in Figure 1. An Ag/AgCl electrode was inserted in each half cell; these electrodes were prepared using the method of Sawyer and Roberts (13). Aqueous NaCl solutions were pumped (160 mL min^{-1}) through each half cell using a Cole-Palmer two-channel Masterflex peristaltic pump; flowing solutions eliminate problems due to concentration polarization at the membrane surfaces (14). Cell potentials were measured using the PARC 273. Raw EMF data were obtained continuously at a rate of 250 points per sec. 97,000 of such raw EMF data points were then averaged to obtain a measured cell potential.

Preparation of NIGT membranes. As-received Gore-tex membrane was cut into $2.5 \times 2.5 \text{ cm}$ squares, cleaned ultrasonically in ethanol, dried in a vacuum oven (110°C), and weighed. A tarred Gore-tex square was then placed in a Petri dish containing 20 mL of a solution of Na^+ -form Nafion in DMSO; the Nafion concentration ranged between 0.001 and 1.34 (w/v) %. The Gore-tex membrane was allowed to equilibrate with the Nafion solution for two hours at room temperature. The Petri dish was then placed in the apparatus shown in Figure 2 for solvent evaporation.

The inner beaker in figure 2 contains DMSO. This inner beaker is placed in an outer beaker which serves as an oil bath. The oil bath was heated to 185° C and the Nafion solution in the Petri dish was evaporated to dryness. The DMSO in the inner beaker insured that the membrane was always in contact with DMSO vapor during the evaporation process (5,8).

After solvent evaporation, the Nafion present on the surfaces of the NIGT membrane was swollen, by immersion in 5 mL of hot (80° C) DMSO, and then wiped away, by scrubbing with a Kimwipe. This procedure insured that the transport properties of the NIGT membrane were not altered by surface layers of conventional Nafion film. The NIGT membrane was then dried in vacuo at 110° C and reweighed. The weight fraction of Nafion in the membrane (defined here as W) was determined by difference; W is given by

$$W = w_n / (w_n + w_g) \quad (1)$$

where w_n and w_g are the weights of Nafion and Gore-tex, respectively.

Several low temperature-cast NIGT membranes were also prepared and evaluated. Nafion solutions in 50:50 ethanol/water were used to prepare these membranes. The ethanol/water was removed at 70° C.

Assessing the rate of cation-transport in NIGT. Cation transport rates were evaluated by measuring apparent diffusion coefficients (D_{app} 's) for the electroactive cation $Ru(NH_3)_6^{3+}$ in the NIGT membranes. The D_{app} values were obtained using a combination of two electrochemical methods - chronocoulometry at a stationary NIGT-coated Pt electrode and hydrodynamic voltammetry at a rotating NIGT-coated electrode (7-9). In both cases, the NIGT-covered working electrode was immersed in a solution 1 mM in $Ru(NH_3)_6^{3+}$ and 0.2 M in NaCl throughout the duration of the experiment. The volume of this solution was sufficiently large such that the $Ru(NH_3)_6^{3+}$ lost, via partitioning into the

membrane, did not significantly alter the solution $\text{Ru}(\text{NH}_3)_6^{3+}$ concentration.

Chronocoulometric data were obtained by stepping the potential of the electrode from 0.0 V (where no $\text{Ru}(\text{NH}_3)_6^{3+}$ reduction occurs) to -0.425 V, where the rate of the reduction reaction in the membrane is diffusion-controlled. The resulting current was integrated (1) to obtain the corresponding charge-time transient. The charge-time data were analyzed via the Anson equation, which can be written (15)

$$Q(t) = \frac{2nFAD_{\text{app}}^{1/2}\alpha C_{\text{Ru},s}t^{1/2}}{\pi^{1/2}} \quad (2)$$

where t is the time after the potential step, $Q(t)$ is the charge, α is the partition coefficient for $\text{Ru}(\text{NH}_3)_6^{3+}$ between the NIGT membrane and the contacting solution phase, A is the area of the Pt electrode, $C_{\text{Ru},s}$ is the concentration of $\text{Ru}(\text{NH}_3)_6^{3+}$ in the solution phase, and the other terms have their usual meanings (15).

According to Equation 2, a plot of $Q(t)$ vs. $t^{0.5}$ will be linear; the product $D_{\text{app}}^{0.5}\alpha$ can be determined from the slope. Equation 2 is only valid when the diffusion layer created at the Pt/membrane interface is much thinner than the NIGT membrane. This was easily achieved for the rather thick (84 μm) membranes investigated here. Analogous potential step data were obtained with the NIGT-covered electrode in contact with supporting electrolyte (0.2 M NaCl). These background transients were subtracted from the transients obtained in the $\text{Ru}(\text{NH}_3)_6^{3+}$ solution.

The voltammetric data were also obtained by stepping the potential to -0.425 V; however, the electrode was rotated and the steady state current (7-9), obtained at long times (70 min), was recorded. The steady state current (i_{ss}) in this experiment is described by (7-9)

$$\frac{1}{i_{ss}} = \frac{\delta_m}{nFAC_{Ru,s}\alpha D_{app}} + \frac{\nu^{1/6}}{0.62nFAD_s^{2/3}\omega^{1/2}C_{Ru,s}} \quad (3)$$

where ω is the rotation rate, δ_m is the thickness of the NIGT membrane, D_s is the diffusion coefficient for $Ru(NH_3)_6^{3+}$ in the contacting solution phase, and the other terms have their usual meanings (7-9).

According to Equation 3, a plot of i_{ss}^{-1} vs $\omega^{-0.5}$ will be linear; the product $D_{app}\alpha$ can be obtained from the intercept (7-9). Because the Anson plot provides $D_{app}^{0.5}\alpha$ and the i_{ss}^{-1} vs $\omega^{-0.5}$ plot provides $D_{app}\alpha$, both D_{app} and α can be evaluated. Rotation rates of 80, 125, 160, 220, 250, 500, 1000, and 1500 RPM were used in these studies.

Evaluating the cation permselectivity of NIGT. A potentiometric experiment was used to obtain cation transference numbers for the NIGT membranes; the following potentiometric cell was used



The potential of this cell (E_{cell}) is given by (16-19)

$$E_{cell} = 2 t_+ RT/F \ln (a_l/a_r) \quad (5)$$

where a_l and a_r are the activities of Na^+ in the aqueous solutions on the left and right hand sides of the NIGT membrane, respectively, and t_+ is the transference number for Na^+ in the membrane.

The concentration of Na^+ on the right hand side of the membrane was held constant at 2 mM; the concentration on the left hand side was varied from 2 mM to 5M. Activities were calculated using activity coefficients taken from Latimer (20).

RESULTS AND DISCUSSION

Physical properties of the NIGT membranes. As indicated in the introduction, Nafion films cast at low-temperatures (less than ca. 130° C) are hard and brittle (4-5). Such films are not useful materials because they shatter during attempts to remove them from the casting surface (4,5). In contrast, high temperature-cast Nafion is pliant and mechanically strong; the high temperature-cast material forms tough, coherent membranes. The reasons for these differences between low temperature and high temperature-cast Nafion have been discussed in detail (5).

Casting temperature has an analogous effect on the properties of NIGT membranes. NIGT membranes formed at 70° C are brittle and crack when flexed. In contrast, NIGT membranes formed at 185° C are pliant and mechanically strong. High-temperature-cast NIGT is clearly a much better membrane material than low temperature cast NIGT.

Uptake of Nafion by Gore-tex. Table I shows the effect of concentration of Nafion, in the solution phase, on the quantity of Nafion incorporated into the high temperature-cast NIGT membranes. The data in Table I seem to indicate that the Gore-tex becomes saturated with Nafion. The one order of magnitude increase in solution concentration, from 0.11 to 1.34 %, causes only an incremental increase in the quantity of Nafion incorporated into the membrane. Furthermore, using a higher Nafion concentration in the loading solution (e.g. 5%) does not yield higher loading levels. Table I also shows that the quantity of Nafion in the Gore-tex membrane can be varied over a substantial range; this is the interesting feature of the composite membrane concept - a variety of (effectively) different membranes can be prepared from the same two component materials.

Migration of the electroactive cation. The Anson equation (Equation 2) assumes that the electroactive cation arrives at the electrode surface by diffusion and not by migration (15). The contribution an ion, j , makes to the migration current is given by (21)

$$i_{m,j} = z_j^2 D_j C_j \frac{F^2 A}{RT} \left(- \frac{\partial \phi(x)}{\partial x} \right) \quad (6)$$

where z_j is the charge, D_j is the diffusion coefficient, and C_j is the concentration of the ion j , and $\partial \phi / \partial x$ is the potential gradient. The contribution of ion j to the migration current can be made negligibly small by making the product $z_j^2 D_j C_j$ smaller than the sum of the $z^2 DC$ terms for all of the other ions in the solution. This is accomplished, for experiments at uncoated electrodes, by adding a high concentration of an inert "supporting" electrolyte (21).

In analogy to the uncoated-electrode case, the Anson equation will only be applicable at the NIGT-coated electrode if the product $9D_{app}C_{Ru,m}$ (where $C_{Ru,m}$ is the concentration of $Ru(NH_3)_6^{3+}$ in the membrane) is much smaller than the sum of the products $z^2 DC$ for all of the other mobile ions in the membrane. We will show, below, that this is true for the membranes investigated here.

Let us assume the worst case scenario - the NIGT membrane is completely cation permselective; thus, Na^+ is the only other mobile ion in the membrane phase. The experiments described below provide $C_{Ru,m}$ and D_{app} . Furthermore, because W (Equation 1) is known, the concentration of Na^+ in the membrane can be calculated. If we assume that the diffusion coefficient for Na^+ in NIGT is the same as its diffusion coefficient in Nafion (22), we find that the product DC for Na^+ in the most permselective NIGT membranes is at least a factor of 30

times higher than the product $9D_{app}C_{Ru,m}$.

The calculations discussed above show that, even in the limit of complete cation permselectivity, $Ru(NH_3)_6^{3+}$'s contribution to the migration current in the membrane is negligibly small. Furthermore, as will be shown below, none of the NIGT membranes prepared here are completely cation permselective in the presence of 0.2 M NaCl (see Figure 9). These calculations and data clearly show that the Anson equation is applicable to all of the NIGT membranes described here.

Diffusion and partition coefficient data. Figure 3 shows a typical Anson plot associated with the reduction of $Ru(NH_3)_6^{3+}$ in a NIGT membrane. As is predicted by Equation 2, this plot is linear (correlation coefficient = 0.999). The product $D_{app}^{0.5}\alpha$ can be obtained from the slopes of such plots.

Figure 4 shows a plot of i_{ss}^{-1} vs. $\omega^{-0.5}$ for $Ru(NH_3)_6^{3+}$ reduction at a typical rotating NIGT-covered electrode. The expected linearity (7-9) is observed at low rotation rates; however, steady-state currents at high rotation rates appear to be too large. We will show, below, that these membranes contain two ion-transporting pathways - an aqueous solution-like pathway, and a Nafion phase pathway (1). The continuous solution-like pathway accounts for the spuriously large steady-state currents, observed at high rotation rates, in Figure 4.

Rotating a planar disk electrode causes a flow of solution normal to (and in the direction of) the electrode surface (23). If a nonporous polymer film covers the electrode, the steady state limiting current at the electrode/film interface will be described by Equation 3. However, if a continuous aqueous pathway is present in the film, then the solution flow directed normal to the membrane surface can be propagated through the membrane and to the substrate

electrode surface. This convective flow of electroactive species through the membrane will cause the steady-state current to be spuriously large.

This convective flow interpretation of the steady-state current data (Figure 4) is corroborated by the voltammograms shown in Figure 5. These voltammograms were obtained at a scan rate of 0.5 V s^{-1} where the diffusion layer created at the electrode/NIGT interface is much thinner than the NIGT membrane. The inner voltammogram was obtained at a stationary electrode, where there is no convective flow; the outer voltammograms were obtained at rotating electrodes. The higher currents obtained at the rotating electrodes show that $\text{Ru}(\text{NH}_3)_6^{3+}$ is being convected through the NIGT membrane.

Fortunately, the contribution of convection to mass transport in the membrane is insignificant at low rotation rates (note linear region in Figure 4). The product $D_{\text{app}}\alpha$ can be determined by extrapolating this linear portion of the curve (vide supra). These data, in conjunction with the chronocoulmetric data, provide D_{app} and α (Table II).

As was observed for the low temperature-cast NIGT (1), the magnitude of the apparent diffusion coefficient is inversely proportional to the quantity of Nafion incorporated into the membrane. However, D_{app} in the membrane with the highest Nafion loading level (10 %) is still ca. one order of magnitude larger than the D_{app} for $\text{Ru}(\text{NH}_3)_6^{3+}$ in homogeneous Nafion (24). Thus, NIGT membranes can support higher rates of ion-transport than conventional, homogeneous Nafion membranes (1,2,25). The relative merits of NIGT vs. conventional Nafion are considered in our discussion of the permselectivity data.

Table II also shows that the aqueous/NIGT partition coefficient for $\text{Ru}(\text{NH}_3)_6^{3+}$ increases with the quantity of Nafion in the membrane phase. A

quantitative model for this observation (and for the inverse relationship between D_{app} and Nafion content) will be presented in the following two sections of this paper.

Quantitative analysis of the diffusion coefficient data. The D_{app} data for the low temperature-cast NIGT membranes (1) were interpreted in terms of a two pathway diffusion model (1,27). As indicated above, these pathways are a Nafion path and an aqueous-like solution path. We have shown that if these pathways are coupled, the following equation applies (1)

$$D_{app} = \left[D_{Ru,n,m} - \frac{D_{Ru,a,m}}{k} - \frac{D_{Ru,a,m}V_v d_p}{kw_h} \right] + \left(\frac{D_{Ru,a,m}V_v d_p}{kw_h} \right) \frac{1}{W} \quad (7)$$

where $D_{Ru,n,m}$ and $D_{Ru,a,m}$ are the diffusion coefficients for $Ru(NH_3)_6^{3+}$ in the Nafion and aqueous phases within NIGT membrane, k is the partition coefficient for $Ru(NH_3)_6^{3+}$ between these two phases within NIGT (1), d_p is the density of Nafion, w_h is the weight of the NIGT membrane and V_v is the total void volume present within the Gore-tex membrane. In contrast, if the diffusion pathways are uncoupled, the following equation applies (1)

$$D_{app}^{1/2} = \left[D_{Ru,n,m}^{1/2} - \frac{D_{Ru,a,m}^{1/2}}{k} - \frac{D_{Ru,a,m}^{1/2}V_v d_p}{kw_h} \right] + \left(\frac{D_{Ru,a,m}^{1/2}V_v d_p}{kw_h} \right) \frac{1}{W} \quad (8)$$

Both Equations 7 and 8 predict that D_{app} will be inversely proportional to W . However, Equation 7 predicts that D_{app} will be linearly related to $1/W$ whereas Equation 8 predicts that $D_{app}^{0.5}$ will be linearly related to $1/W$. The corresponding plots are shown in Figures 6 and 7. The experimental data fit the coupled diffusion model (Figure 6) and not the uncoupled model (Figure 7). Analogous results were obtained from the low temperature-cast NIGT membranes.

Quantitative analysis of the partition coefficient data. A similar analysis

can be applied to the partition coefficient data shown in Table II. The partition coefficient, α is given by

$$\alpha = C_{Ru,m}/C_{Ru,s} \quad (9)$$

$C_{Ru,m}$ can be broken up into the concentration of $Ru(NH_3)_6^{3+}$ in the Nafion phase within the NIGT membrane, $C_{Ru,n,m}$, and the concentration of $Ru(NH_3)_6^{3+}$ in the solution phase within the membrane, $C_{Ru,a,m}$.

$$C_{Ru,m} = \frac{C_{Ru,a,m} V_{a,m} + C_{Ru,n,m} V_{n,m}}{V_v} \quad (10)$$

where $V_{a,m}$ and $V_{n,m}$ are the volumes of the aqueous and Nafion phases, respectively, within the NIGT membrane.

The total available void volume in the Gore-tex membrane is given by $V_v = V_{a,m} + V_{n,m}$. Furthermore the concentration of $Ru(NH_3)_6^{3+}$ in the aqueous and Nafion phases within the membrane are related by $C_{Ru,n,m} = kC_{Ru,a,m}$, where k is the partition coefficient of $Ru(NH_3)_6^{3+}$ between the aqueous and Nafion phases within NIGT (1). Combining these two equations with Equation 10 and rearranging (28) gives

$$C_{Ru,m} = \frac{C_{Ru,a,m} (V_v + kV_{n,m})}{V_v} \quad (11)$$

Dividing both sides of Equation 11 by $C_{Ru,s}$ gives

$$\alpha = \frac{C_{Ru,a,m}(V_v + kV_{n,m})}{V_v C_{Ru,s}} \quad (12)$$

Equation 1 can be rearranged to $w_n = w_s[W/(1-W)]$. Furthermore, the volume of Nafion present is given by $V_{n,m} = w_n/d_n$, where d_n is the density of Nafion. Combining these two equations gives

$$V_{n,m} = \frac{w_s}{d_n} \frac{W}{(1-W)} \quad (13)$$

Substituting Equation 13 into Equation 12 and rearranging gives

$$\alpha = \frac{C_{Ru,a,m}}{C_{Ru,s}} \frac{V_v}{V_m} + \frac{C_{Ru,a,m} k w_s}{C_{Ru,s} V_m d_n} \frac{W}{(1-W)} \quad (14)$$

According to Equation 14, α should be linearly related to the parameter $[W/(1-W)]$. Figure 8 shows the partition coefficient data plotted as per Equation 14; this plot is, indeed, linear (correlation coefficient = 0.997). These data provide support for the validity of Equation 14 and further support for the two pathway model.

Transference number data. The D_{app} data indicate that NIGT can support higher rates of ion-transport than homogeneous Nafion membrane. In many applications, however, selectivity is just as important as rate of ion-transport. We did not address the issue of cation-transport selectivity (i.e. cation permselectivity) in our previous paper (1). Cation permselectivity was evaluated, for both low and high-temperature cast NIGT membranes, as part of the investigation discussed in this paper.

Figure 9 provides a qualitative picture of the cation permselectivities of high-temperature-cast NIGT. The dashed curve in Figure 9 was calculated from Equation 5, assuming a cation transference number of unity (ideal cation permselectivity). The upper most solid curve is experimental data from a homogeneous Nafion membrane. Nafion is one of the most cation-permselective materials known (29); this is reflected in the enormous concentration range over which the Nafion data fall on the ideally cation permselective line.

Figure 9 shows that the cation permselectivity of NIGT increases with the quantity of Nafion incorporated into the membrane. The NIGT membrane

containing 10 % Nafion is almost as permselective as homogeneous Nafion; furthermore, recall that D_{app} for this membrane is an order of magnitude higher than the corresponding D_{app} in homogeneous Nafion. These data suggest that the NIGT membrane containing 10 % Nafion would, for some applications, be superior to Nafion. This would be especially true in applications where transport selectivity could be sacrificed for transport facility.

Cation permselectivity is expressed, in quantitative terms, by the cation transference number (t_+ , Equation 5). Transference numbers for the various NIGT membranes are presented in Table II. Again, these data show that cation permselectivity increases with the quantity of Nafion incorporated into the membrane, and that the permselectivity of the 10 %-loaded membrane is excellent.

A simple, physical picture of the two pathway diffusion model. The following statement may not be universally true, but it seems to be the general case - Highly selective membranes usually show low rates of mass transport and poorly selective membranes usually show higher rates of mass transport (30). The data obtained here adhere to this statement (compare D_{app} and t_+ columns in Table II). The following simple, physical picture of the two-pathway diffusion model can be used to account for these data.

Gore-tex is a random, tortuous pore material; electron micrographs (12) show that the dimensions of the internal void spaces vary over a large range. Gas-transport measurements can, however, provide a "mean" diameter for the various tortuous pores in Gore-tex. The membranes described, thus far, had mean pore diameters of 20 nm.

The most rudimentary model for Gore-tex is, therefore, a collection of pores, with a broad distribution of diameters, and a mean diameter of 20 nm.

The most rudimentary model for NIGT assumes that the walls of these pores are coated with Nafion. This model is supported by electron micrographic evidence (12). At the relatively low Nafion-loading levels discussed here, the majority of the pores will not be completely filled with Nafion; i.e. the pores will contain a hollow core (Figure 10 A). This model is also supported by electron micrographic data (12).

Upon exposure to aqueous solution, the hollow core at the center of the Nafion-coated pore fills with water. These water-filled cores provide the solution-like pathway for ion-transport. Whether excess electrolyte also enters a pore will depend on the thickness of the Nafion layer and the thickness of the double layer at the Nafion/solution interface. The thickness of the Nafion layer increases with the Nafion-loading level. The double layer thickness varies with the electrolyte concentration (31).

Consider two simple limiting cases. First, assume that the NIGT membrane is loaded to the highest level investigated here (10%). In this case, the Nafion film which coats the pore wall will be relatively thick. This leaves a very narrow hollow core. Upon exposure to water, the ionic double layer completely fills this core (symbolized by horizontal lines in (Figure 10B)). Because the double layer completely fills the core, anions are excluded from the pore. If enough (vide infra) of these anion-blocking pores are present in the NIGT membrane, the entire membrane will, likewise, block anion-transport. A cation transference number of unity will be obtained.

Now, assume that the Nafion loading level is extremely low (e.g. 1 %) so that the Nafion film which coats the pore wall is very thin. This leaves a very wide hollow core. Upon exposure to water, an ionic double layer again forms but the double layer can not completely fill this core (Figure 10C). In

this case, anions (i.e. excess electrolyte) are not excluded from the pore. If enough of these anion-passing pores are present in the NIGT membrane, the entire membrane will, likewise, pass anions and the cation transference number will be less than unity.

The above examples are the limiting cases. Suppose that the Nafion film thickness in a pore is such that at low electrolyte concentrations (where the ionic double layer is thick (31)), the double layer completely fills the hollow core, whereas at high electrolyte concentrations (where the ionic double layer is thin (31)), the double layer only partially fills the core. In this case, the membrane will reject anions at low electrolyte concentrations and pass anions at high electrolyte concentrations. This is precisely the experimental observable for NIGT membranes with intermediate Nafion-loading levels (Figure 9).

This simple coated-pore model can, therefore, qualitatively account for the effect of Nafion loading-level on the cation permselectivity of NIGT membranes. A further (and rather stringent) test of this model can be devised. Depending on the electrolyte concentration, the ionic double layer can be anywhere from several tenths of nm's to perhaps as much as 10 nm's in thickness (31). Fortuitously, this is approximately the thickness regime needed to block anion-transport in the pores of the 20 nm pore-diameter NIGT membrane. However, even the thickest double layer would not be able to block anion-transport in a 200 nm pore-diameter membrane. Thus, a membrane based on 200 nm mean pore-diameter Gore-tex would never show good cation permselectivity.

To test this hypothesis we compared cation transference numbers for membranes based on the 20 nm mean pore-diameter material with analogous

transference numbers for membranes based on 200 nm mean pore-diameter Gore-tex. In this case the membranes were prepared using the low temperature casting procedure; the data obtained are shown in Table III. In agreement with the above prediction, the membranes based on the 200 nm pore-diameter material never show high cation transference numbers. In contrast, the membranes based on the 20 nm pore diameter Gore-tex can, at high Nafion loading levels, show excellent cation permselectivities.

CONCLUSIONS

High temperature-cast NIGT membranes show better mechanical properties than the low temperature-cast membranes discussed in our previous paper (1). The two diffusion-pathway model, described earlier, quantitatively accounts for the transport data for the high temperature-cast membranes. At the ca. 10 percent (or higher) Nafion loading-level, both the high and low temperature-cast membranes show excellent cation permselectivity. Furthermore these membranes show cation-transport rates for $\text{Ru}(\text{NH}_3)_6^{3+}$ which are an order of magnitude higher than transport rates in homogeneous Nafion.

NIGT can achieve high cation-transport rates and relatively high cation permselectivities. It is interesting to speculate how this is achieved in NIGT membranes. One possible answer is that, because the pores are interconnected, all of the large (unblocked) pores ultimately feed into very small (anionically-blocked) capillaries. As a result, an anion attempting to traverse the membrane will ultimately run into an anionically-blocked pore; therefore, the membrane cannot transport anions.

Electron micrographs show that the majority of the Nafion in NIGT is coated along the walls of the large (unblocking) pores (12). If the argument presented above is correct, then the majority of the Nafion in the NIGT

membrane is not actively involved in the anion rejection process. Since Nafion is a very expensive material, this is an undesirable situation. The solution to this problem is obvious - rather than dispersing a relatively large quantity of Nafion throughout the membrane (where most of it is not involved in the anion rejection process), disperse a much smaller quantity of Nafion as an ultrathin film on one face of the membrane. We are currently pursuing this goal.

Acknowledgements. This work was supported by the Air Force Office of Scientific Research and the Office of Naval Research.

REFERENCES

1. C. Liu and C. R. Martin, *J. Electrochem. Soc.* 137, 510, (1990).
2. R.M. Penner and C.R. Martin, *J. Electrochem. Soc.* 132, 514, (1985).
3. A. Eisenberg and H.L. Yeager, *Perfluorinated Ionomer Membranes*, ACS Symposium series 180. Washington, DC. 1982.
4. R.B. Moore, III and C.R. Martin, *Macromolecules*, 22, 3594 (1989).
5. R.B. Moore III and C.R. Martin, *Macromolecules*, 21, 1334, (1988).
6. R.B. Moore, III and C.R. Martin, *Anal. Chem.*, 56, 2569 (1989).
7. C.A. Marrese, O. Miyawaki, and L.B. Wingard, Jr. *Anal. Chem.*, 59, 248, (1987).
8. D.R. Lawson, L.D. Whitely, C.R. Martin, M.N. Szentirmay, and J.I. Sung, *J. Electrochem. Soc.* 1988, 135, 2247.
9. D.A. Gough and J.K. Laypoldt, *Anal. Chem.* 51, 439, (1979).
10. M.G.A. Khedr, S.M. Abdel Haleem, and A. Baraka, *J. Electroanal. Chem.* 182, 157, (1985).
11. C.R. Martin, T.A. Rhoads, and J.A. Ferguson, *Anal. Chem.* 54, 1639, (1982).
12. R.M. Penner and C.R. Martin, *J. Electrochem. Soc.* 133, 310, (1986).
13. D.T. Sawyer and J.L. Roberts, Jr. "Experimental Electrochemistry for Chemists", John Wiley & Sons: New York, 1974; p 40.
14. G. Tiravanti and R. Passino, *J. Memb. Sci.* 13, 349, (1983).
15. A. J. Bard and L.R. Faulkner, "Electrochemical Methods", John Wiley: New York, 1980, p. 200.
16. N. Lakshminarayanaiah, *J. Phys. Chem.* 73, 1, (1969).
17. N.W. Rosenberg, J.H.B. George, and W.D. Potter, *J. Electrochem. Soc.* 104, 111, (1957).

18. T.M. Ellison and H.G. Spencer, *J. Polym. Sci. B1*, 707, (1963).
19. D.K. Hale and D.J. Mccauley, *Trans Faraday Soc.* 57, 135, (1961).
20. W.M. Latimer "Oxidation Potential", Prentice-Hall:New York, 1952; p. 354.
21. A. J. Bard and L.R. Faulkner, "Electrochemical Methods", John Wiley: New York, 1980, pp. 121-127.
22. H.L. Yeager and B. Kipling *J. Phys. Chem.* 83, 1836, (1979).
23. A.J. Bard and L.R. Faulkner, "Electrochemical Methods", John Wiley: New York, 1980, p. 287.
24. C.R. Martin and Kirt. Dollar, *J. Electroanal. Chem.* 159, 127 (1983).
25. In a recent paper (26) we measured conductivities of NIGT membranes. The conductivities were lower than the conductivity of homogeneous Nafion membrane. However, a solid state electrochemical cell was used for these (26) measurements, and the charge carrying ion was not rather than $\text{Ru}(\text{NH}_3)_6^{3+}$, which was used here. Thus, direct comparisons between these data and the data obtained here are difficult.
26. Z. Cai, C. Liu, and C.R. Martin, *J. Electrochem. Soc.* 136, 3356 (1989).
27. C.J. Miller and M. Majda, *J. Electroanal. Chem.* 207, 49, (1986).
28. In rearranging the assumption is made that $kV_{n,m} \gg V_{n,m}$. As indicated in (1), this is clearly valid.
29. W.Y. Hsu and T.D. Gierbe, in "Perfluorinated Ionomer Membranes." A. Eisenberg and W.L. Yeager, Eds. ACS Symp. Series 180, 1982 P. 283.
30. J.Y. Lai, Y. Sumito, K. Kamide, and S.J. Mauabe, *J. Appl. Polym. Sci.* 32, 4225 (1986).
31. J. O'M. Bockris and A.K.N. Reddy "Modern Electrochemistry," Plenum/Rose Ha NY, 1970, Vol. Chap. 3.3.

Table I. The effect of concentration of Nafion in the solution phase on weight fraction of Nafion incorporated into high temperature-cast NIGT membranes.

Concentration of Nafion Solution ¹ % w/v	Volume of Nafion Solution mL	% Nafion (w/w) in NIGT membranes ² % w/w
0.001	20.0	1.48
0.005	20.0	2.20
0.010	20.0	4.36
0.110	20.0	7.37
1.340	20.0	9.98

1. The solvent is DMSO.

2. Nafion was impregnated in 20 nm mean pore diameter Gore-tex via high temperature method.

Table II. The effect of weight fraction of Nafion in the NIGT membrane on diffusion coefficient, partition coefficient, and transference number.

% Nafion (w/w) in NIGT membrane ¹ % w/w	Diffusion Coefficient ² $\times 10^7 \text{ cm}^2/\text{s}$	Partition Coefficient ³	Transference Number ⁴
1.48	7.7	3.2	0.40
2.20	5.5	6.1	0.61
4.36	2.2	11.3	0.77
7.37	1.8	20.2	0.80
9.98	1.1	25.9	0.97

1. Nafion was impreganted in 20 nm mean pore diameter Gore-Tex via high temperature method.
2. The apparent diffusion coefficients of $\text{Ru}(\text{NH}_3)_6^{3+}$ in the NIGT membrane.
3. The partition coefficient of $\text{Ru}(\text{NH}_3)_6^{3+}$ between the NIGT membrane and the external solution, which was 1mM $\text{Ru}(\text{NH}_3)_6^{3+}$ and 0.2M NaCl.
4. The transference number of Na^+ in the NIGT membrane. The solutions on either side of the membrane were 0.02M NaCl and 0.08 M NaCl.

Table III. The effect of pore size and the % Nafion in the membrane on cation transference number of NIGT¹

200 nm mean pore diameter		20 nm mean pore diameter	
% Nafion (w/w) in NIGT membrane	t_+	% Nafion (w/w) in NIGT membrane	t_+
1.3	0.40	8.5	0.74
10.9	0.56	10.0	0.95
13.5	0.61	12.5	0.99

1. Membranes prepared by low temperature solution casting method.

FIGURE CAPTIONS

- Figure 1.** Schematic of electrochemical cell for measuring EMF's. a. Ag/AgCl electrode; b. Membrane; c. Solution outlet; d. Teflon half-cell; e. Solution inlet; g. Hand wheel; h. Cell holder.
- Figure 2.** Schematic of apparatus used for high temperature solution casting. a. DMSO; b. DMSO solution of Nafion; c. Membrane; d. Oil bath; e. Thermometer; f. Cell holder; g. Stirring bar.
- Figure 3.** A typical Anson plot for the reaction of $\text{Ru}(\text{NH}_3)_6^{3+}$ in NIGT (9.98% Nafion). The contacting solution contained 1mM $\text{Ru}(\text{NH}_3)_6^{3+}$ and 0.2M NaCl.
- Figure 4.** A typical i_{ss}^{-1} vs $\omega^{-0.5}$ (see text) plot for the reduction of $\text{Ru}(\text{NH}_3)_6^{3+}$ in NIGT (9.98% Nafion); contacting solution as per Figure 3.
- Figure 5.** Cyclic voltammograms for $\text{Ru}(\text{NH}_3)_6^{3+}$ in NIGT (9.98% Nafion; contacting solution as per Figure 3. Scan rate: 500mV/s. Rotating rate: --- 0 RPM; $\Delta\Delta\Delta$ 500 RPM; $\circ\circ\circ$ 3000 RPM.
- Figure 6.** Plot of D_{app} vs. $1/W$ (see text) for high temperature-cast membranes.

Figure 7. Plot of $D_{app}^{1/2}$ vs. $1/W$ (see text) for high temperature-cast membranes.

Figure 8. Plot of α vs. $W/(1-W)$ for high temperature-cast membranes.

Figure 9. Potentiometric data plotted as per Equation 5. (-----) calculated via Equation 5 assuming $t_+ = 1$; (ooooo) homogeneous Nafion membrane. The other data are for high temperature cast NIGT membranes. (•••••) 9.98% Nafion; (•••••) 7.37% Nafion; (■ ■ ■ ■) 4.36% Nafion; (◆◆◆◆) 1.48% Nafion.

Figure 10. A simplified representation of the two pathway diffusion model.

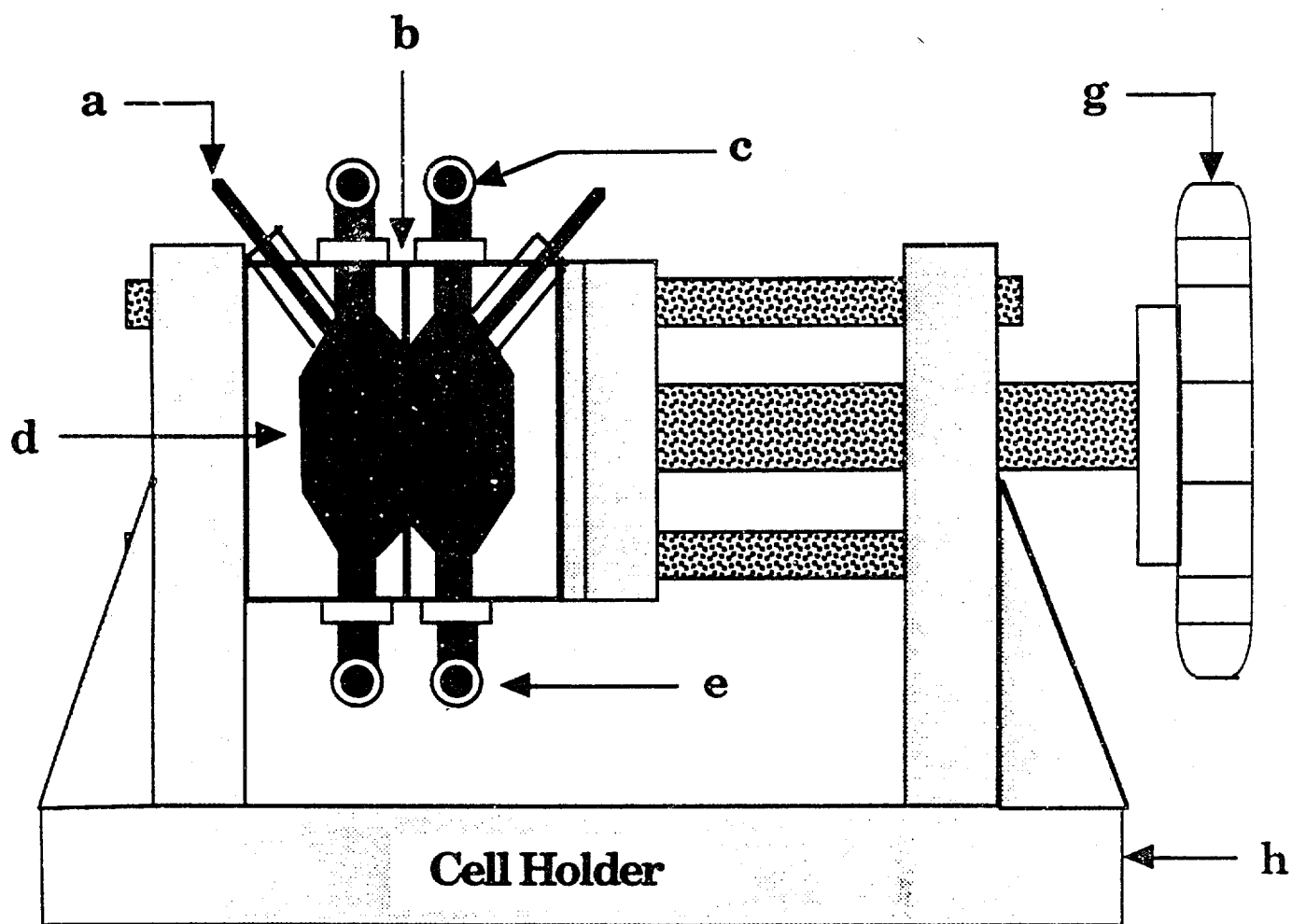


Fig 1

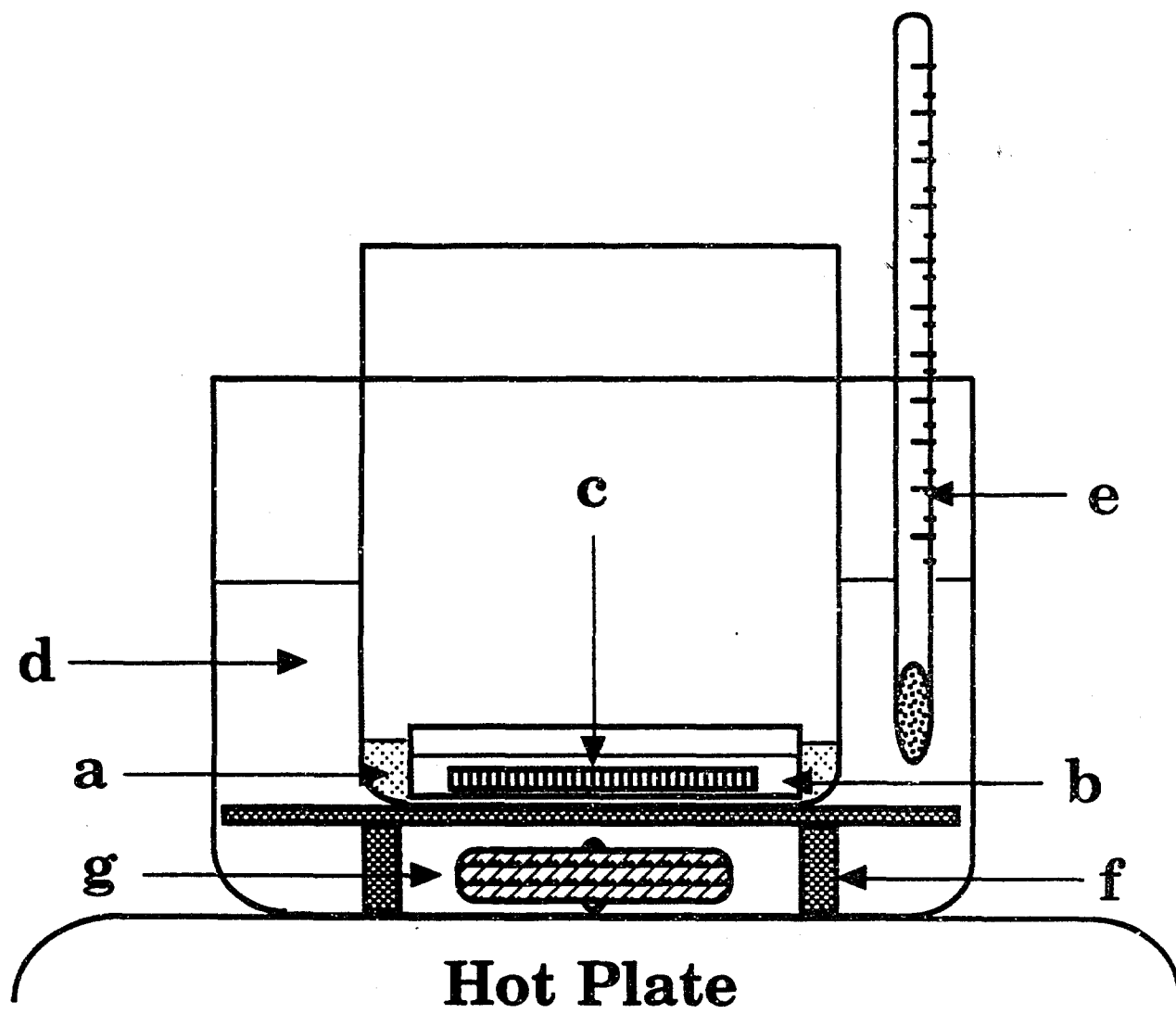


Fig. 2

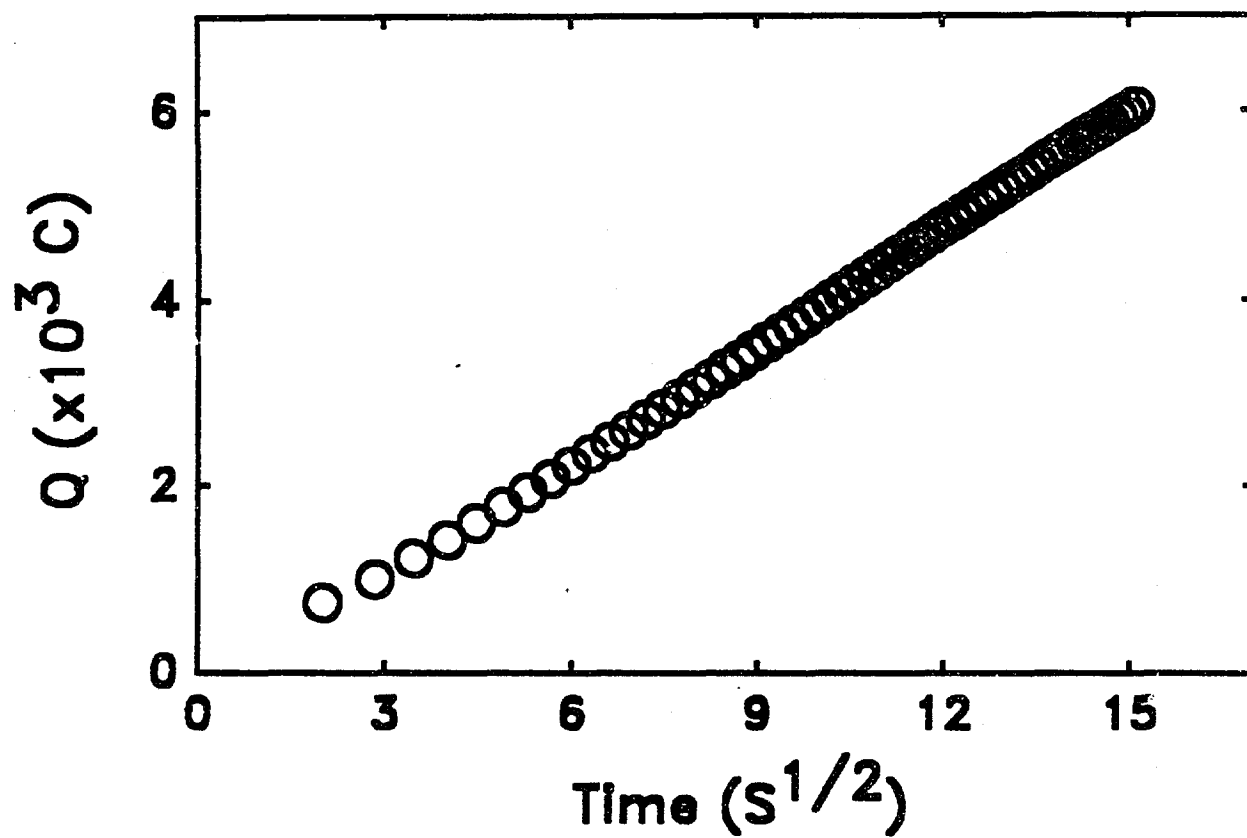


Fig. 3

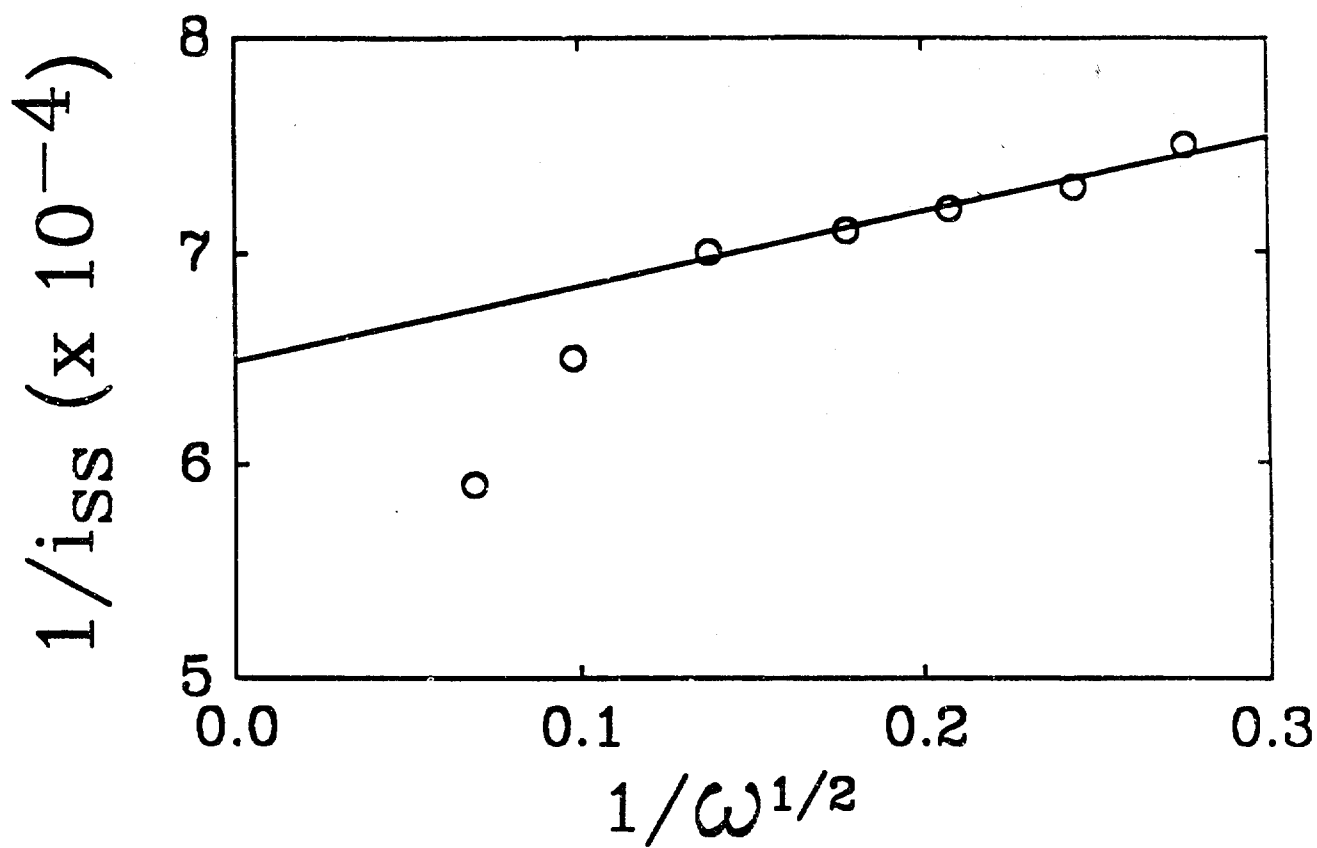


Fig 4

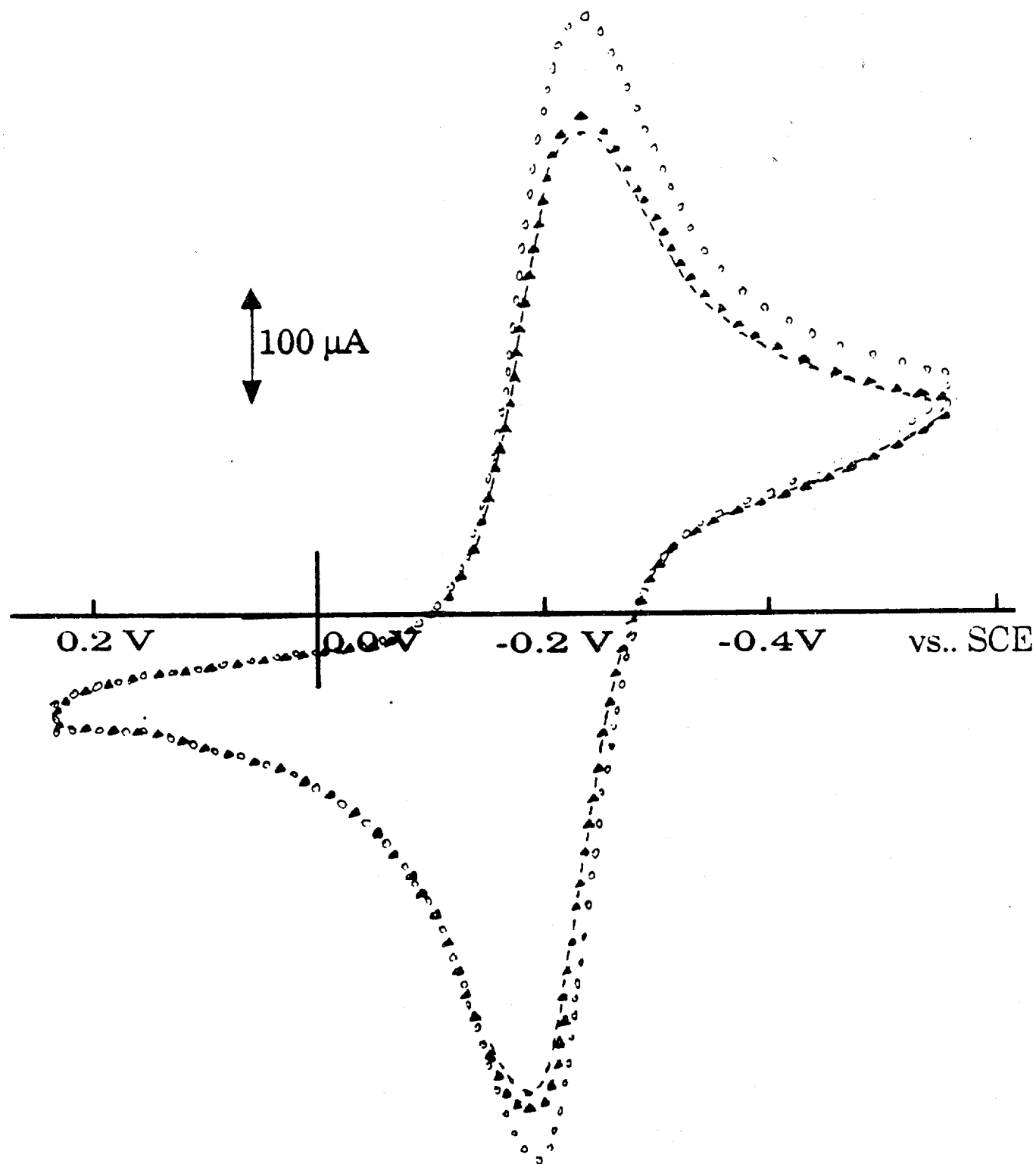


Fig 5

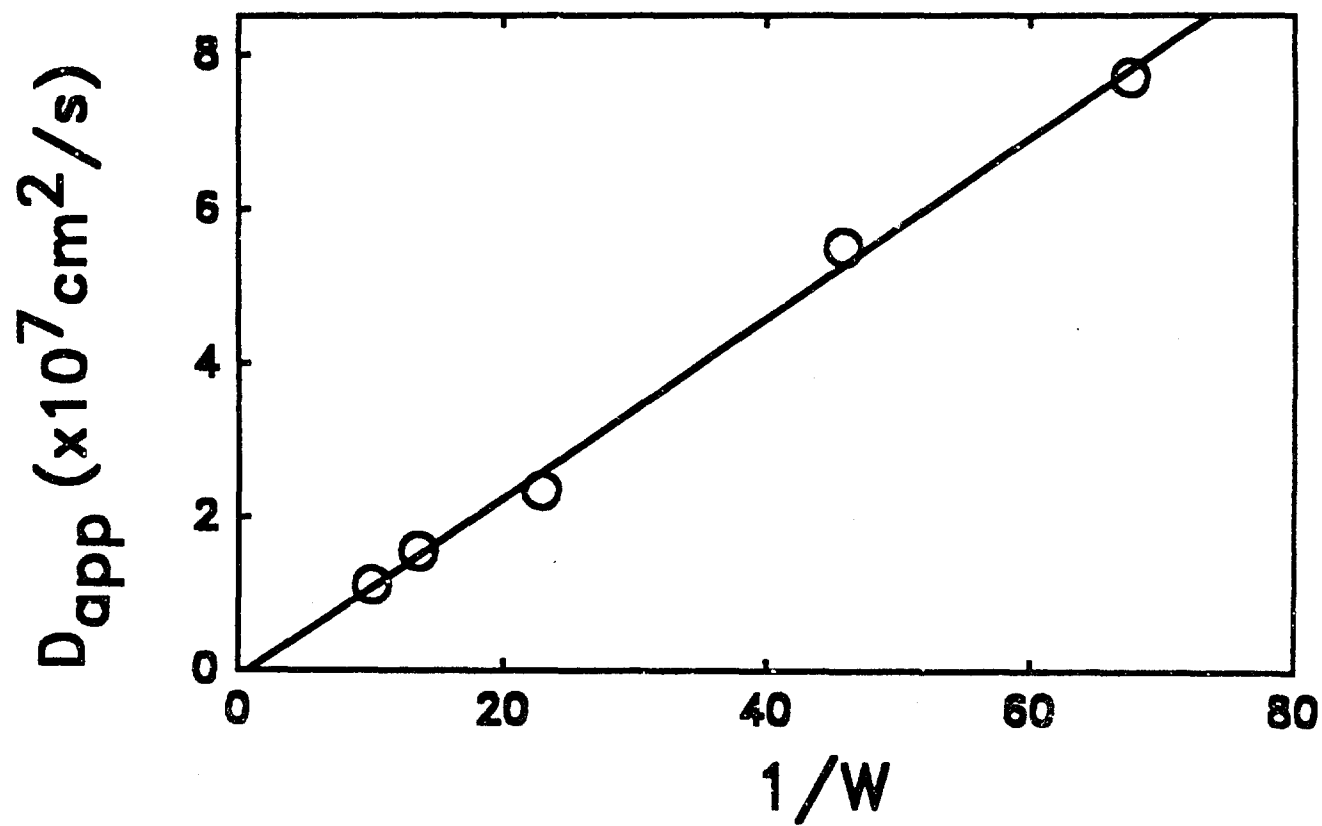


Fig 6

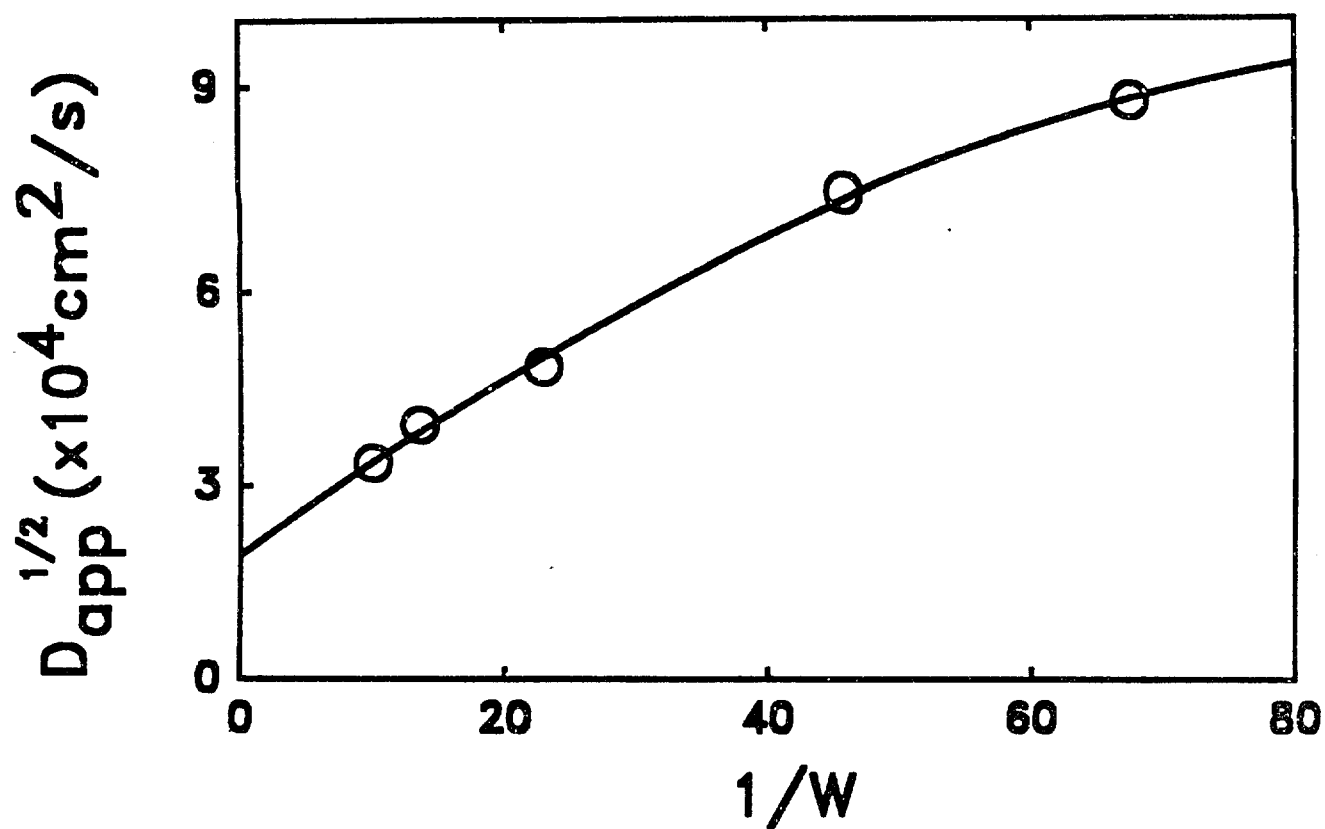


Fig 7

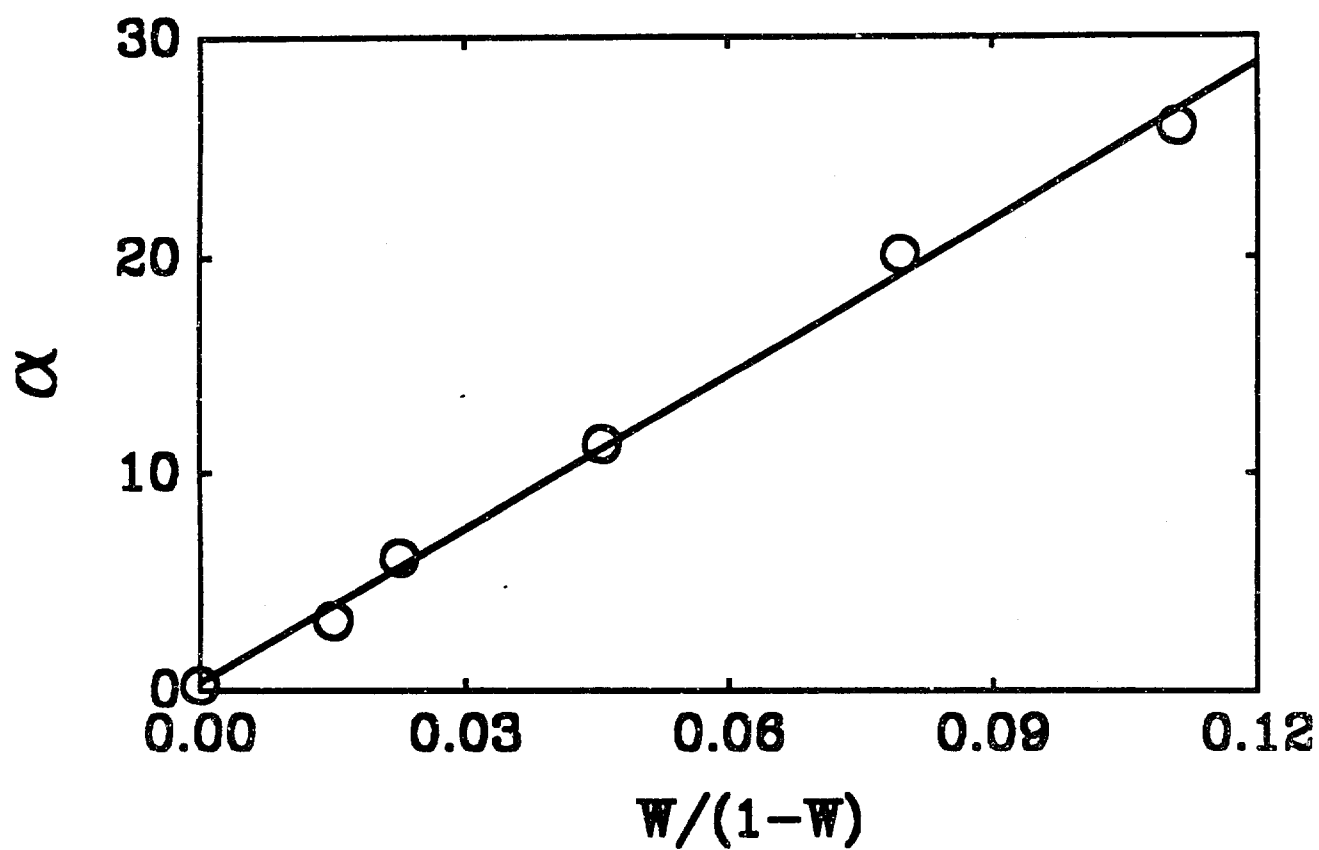


Fig 8

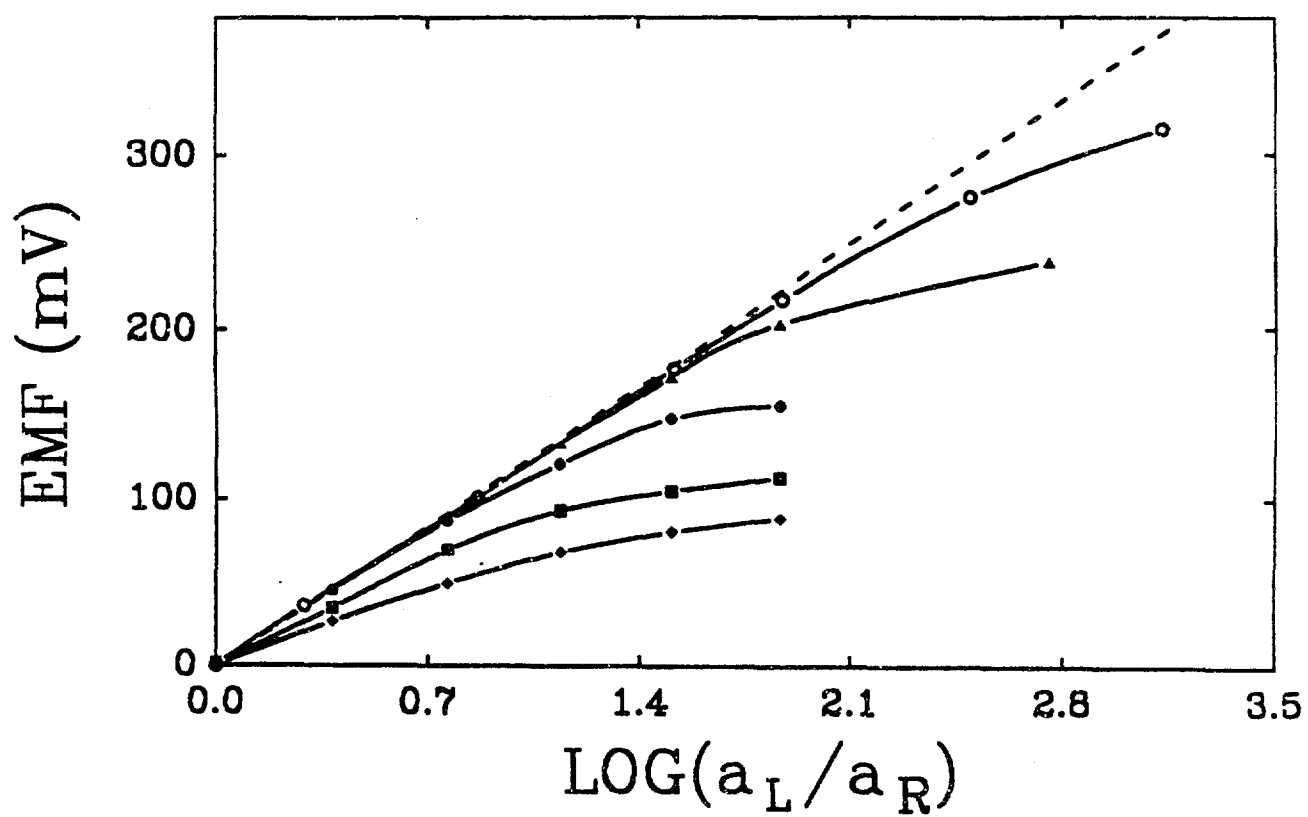


Fig 9